




CLINICAL REPORT

Multisystem disorder associated with a pathogenic variant in *CLCN7* in the absence of osteopetrosis

Chung-Lin Lee^{1,2,3,4,5}  | Yeun-Wen Chang^{1,6} | Hsiang-Yu Lin^{1,3,4,5,7,8}  |
Hung-Chang Lee¹  | Ting-Chi Yeh¹ | Li-Ching Fang¹ | Ni-Chung Lee⁹ |
Jeng-Daw Tsai^{1,4} | Shuan-Pei Lin^{1,3,4,7,10}

¹Department of Pediatrics, MacKay Memorial Hospital, Taipei, Taiwan

²Department and Institute of Clinical Medicine, National Yang-Ming Chiao-Tung University, Taipei, Taiwan

³Department of Rare Disease Center, MacKay Memorial Hospital, Taipei, Taiwan

⁴Department of Medicine, Mackay Medical College, New Taipei City, Taiwan

⁵Mackay Junior College of Medicine, Nursing, and Management, Taipei, Taiwan

⁶Department of Pediatrics, Taipei Tzu Chi Hospital, Buddhist Tzu Chi Medical Foundation, New Taipei City, Taiwan

⁷Division of Genetics and Metabolism, Department of Medical Research, MacKay Memorial Hospital, Taipei, Taiwan

⁸Department of Medical Research, China Medical University Hospital, China Medical University, Taichung, Taiwan

⁹Department of Pediatrics, National Taiwan University Hospital, Taipei, Taiwan

¹⁰Department of Infant and Child Care, National Taipei University of Nursing and Health Sciences, Taipei, Taiwan

Correspondence

Jeng-Daw Tsai and Shuan-Pei Lin,
Department of Pediatrics, MacKay
Memorial Hospital, No. 92, Sec. 2,
Chung-Shan North Road, Taipei 10449,
Taiwan.

Email: tsajjd@yahoo.com.tw and
4535lin@gmail.com

Funding information

Mackay Memorial Hospital, Grant/
Award Number: MMH-E-111-13,
MMH-E-112-13, MMH-MM-112-14,
MMH-MM-113-13 and MMH-E-113-13;
National Science and Technology
Council, Grant/Award Number: NSTC-
110-2314-B-195-010-MY3, NSTC-110-
2314-B-195-014, NSTC-110-2314-B-
195-029, NSTC-111-2314-B-195-017,
NSTC-111-2811-B-195-001, NSTC-111-
2811-B-195-002, NSTC-112-2314-B-
195-003, NSTC-112-2314-B-195-014-
MY3 and NSTC-112-2811-B-195-001

Abstract

Background: We clinically and genetically evaluated a Taiwanese boy presenting with developmental delay, organomegaly, hypogammaglobulinemia and hypopigmentation without osteopetrosis. Whole-exome sequencing revealed a de novo gain-of-function variant, p.Tyr715Cys, in the C-terminal domain of CIC-7 encoded by *CLCN7*.

Methods: Nicoli et al. (2019) assessed the functional impact of p.Tyr715Cys by heterologous expression in *Xenopus* oocytes and evaluating resulting currents.

Results: The variant led to increased outward currents, indicating it underlies the patient's phenotype of lysosomal hyperacidity, storage defects and vacuolization. This demonstrates the crucial physiological role of CIC-7 antiporter activity in maintaining appropriate lysosomal pH.

Conclusion: Elucidating mechanisms by which *CLCN7* variants lead to lysosomal dysfunction will advance understanding of genotype–phenotype correlations. Identifying modifier genes and compensatory pathways may reveal therapeutic targets. Ongoing functional characterization of variants along with longitudinal clinical evaluations will continue advancing knowledge of CIC-7's critical roles and disease mechanisms resulting from its dysfunction. Expanded cohort studies are warranted to delineate the full spectrum of associated phenotypes.

This is an open access article under the terms of the [Creative Commons Attribution-NonCommercial-NoDerivs](https://creativecommons.org/licenses/by-nc-nd/4.0/) License, which permits use and distribution in any medium, provided the original work is properly cited, the use is non-commercial and no modifications or adaptations are made.

© 2024 The Author(s). *Molecular Genetics & Genomic Medicine* published by Wiley Periodicals LLC.

KEYWORDS

albinism, *CLCN7* variant, hypogammaglobulinemia, lysosomal acidification

1 | INTRODUCTION

Lysosomes are membrane-bound intracellular organelles containing hydrolase enzymes that catalyze macromolecule degradation and recycling of constituents in cells. Maintaining an acidic luminal pH is essential for optimal lysosomal function (Hamer et al., 2012). Active proton accumulation in lysosomes is primarily driven by the vacuolar-type H⁺-ATPase (V-ATPase) proton pump, but acidification also necessitates counterion movement to preserve electroneutrality (Mindell, 2012; Xiong & Zhu, 2016). Defects in ion channels or transporters regulating counterion flux can disrupt homeostasis and eventually lead to pathologies including neurodegeneration and lysosomal storage diseases (Devuyst et al., 1999; Kasper et al., 2005; Mohammad-Panah et al., 2002; Poët et al., 2006; Stobrawa et al., 2001). Chloride is considered the primary counterion traversing the lysosomal membrane (Graves et al., 2008) via the chloride/proton exchanger CLC-7, encoded by *CLCN7*. However, CLC-7's precise role in acidification remains contentious, with some studies supporting its involvement while others question it (Graves et al., 2008; Kasper et al., 2005; Kornak et al., 2001; Majumdar et al., 2011; Steinberg et al., 2010; Weinert et al., 2010).

Lange et al. (2006) demonstrated by immunofluorescence colocalization that *CLCN7* and *OSTM1* proteins are both localized to late endosomes, lysosomes, and specifically the ruffled border of bone-resorbing osteoclasts in various mammalian tissues. Coimmunoprecipitation experiments showed that *CLCN7* and *OSTM1* physically interact and form a molecular complex, suggesting *OSTM1* functions as a β subunit of *CLCN7* to regulate its localization and activity. Additional experiments revealed *CLCN7* is required to transport *OSTM1* to the lysosome, where the highly glycosylated luminal domain of *OSTM1* undergoes proteolytic processing into its mature form. Gray-lethal mice, which lack the *Ostm1* gene, exhibited greatly reduced *Clcn7* protein levels but normal *Clcn7* RNA levels in tissues, indicating the *Clcn7*-*Ostm1* protein-protein interaction is important for *Clcn7* protein stability.

Quantification showed *Clcn7* protein levels in *Ostm1*-deficient tissues and cells, including osteoclasts, were less than 10% of normal levels, leading to the conclusion that *Ostm1* mutations likely cause osteopetrosis primarily by impairing acidification of the osteoclast resorption lacuna which is dependent on *Clcn7*. The similar lysosomal storage pathology and neurodegeneration seen in both gray-lethal and *Clcn7* knockout mice implies the *Clcn7*-*Ostm1*

protein complex has a broader importance beyond bone homeostasis (Lange et al., 2006).

Graves et al. (2008) directly measured and characterized an anion transport pathway in purified lysosomes, demonstrating it has the expected characteristics of a CLC-type Cl⁻/H⁺ antiporter. Additional experiments silencing *Clc7* gene expression showed this transporter constitutes the major route for chloride ion flux across the lysosomal membrane. Knockdown of *Clc7* expression using short interfering RNA substantially ablated the lysosomal Cl⁻/H⁺ antiport activity and strongly reduced the ability of lysosomes to acidify in vivo. Taken together, they concluded *CLC7* functions as a Cl⁻/H⁺ antiporter that comprises the predominant Cl⁻ permeability pathway in lysosomes and is vital for normal lysosomal acidification (Graves et al., 2008).

Patients with loss-of-function mutations in *CLCN7* can develop either autosomal dominant osteopetrosis type 2 (OPTA2; OMIM 166600) or autosomal recessive osteopetrosis type 4 (OPTB4; OMIM 611490), depending on the specific mutation and inheritance pattern (Jentsch, 2007; Jentsch et al., 2005). These disorders highlight the importance of *CLCN7* for normal bone homeostasis and modeling. We present a case report of a child who harbors a confirmed pathogenic de novo variant in *CLCN7* that manifested not with osteopetrosis but rather as a more complex pleiotropic syndrome comprising of cutaneous albinism, developmental delay, organomegaly, enteropathy, and hypogammaglobulinemia. The de novo missense variant c.2144A>G (p.Tyr715Cys) (GenBank: NM_001287.5) (ClinVar: RCV000412760.1) found in the proband was shown by functional studies to result in increased chloride flux mediated by CLC-7, reflecting a gain-of-function effect (Nicoli et al., 2019). Additional functional assays revealed this variant decreased lysosomal pH and induced enlarged cytoplasmic vacuoles in patient-derived fibroblasts. A mouse model engineered to carry a corresponding heterozygous variant likewise displayed hallmarks of lysosomal dysfunction including hypopigmentation, organomegaly, and lysosomal storage, providing further evidence that the p.Tyr715Cys variant is pathogenic and disrupts normal *CLCN7* function (Nicoli et al., 2019). Moreover, the increased cellular acidity and abnormal cellular phenotype observed in the proband's cells was able to be reversed in vitro upon treatment with the lysosomotropic alkalinizing agent chloroquine, pharmacologically highlighting that CLC-7 plays an integral role in controlling lysosomal pH homeostasis (Nicoli et al., 2019).

A recent study by Bose et al. (2023) investigated the effects of the gain-of-function *CLCN7* variant p.Tyr715Cys on lysosomal acidification and function. They found that expression of this variant in HeLa cells led to enlarged cytoplasmic vacuoles derived from endo-lysosomes. These vacuoles exhibited defective proteolytic capacity, with reduced degradation of endocytosed proteins. Additionally, expression of the p.Tyr715Cys variant resulted in impaired autophagic clearance, with increases in the autophagy markers LC3-II and p62 indicating a buildup of autophagic material. Their results demonstrate that dysregulated lysosomal pH homeostasis due to enhanced CLC-7 antiporter activity can profoundly disrupt cellular processes.

2 | MATERIALS AND METHODS

2.1 | Patient

A 25-month-old Taiwanese male presented clinically with generalized hypopigmentation of the skin, hair, and ocular albinism that had been present since birth (Figure 1a).

Additional medical history revealed failure to thrive, significant developmental delays, and organomegaly upon physical exam. The patient exhibited protein-losing enteropathy that required placement of a percutaneous endoscopic gastrostomy tube to provide supplemental nutritional support. An abdominal ultrasound showed diffuse and homogeneous increased echogenicity throughout the liver parenchyma, indicating suspected inflammation and liver dysfunction (Figure 1b). Renal ultrasound revealed nephromegaly affecting both kidneys, with increased cortical echogenicity and poor corticomedullary differentiation (Figure 1c), suggestive of a renal tubulointerstitial process. Brain magnetic resonance imaging revealed a mild prominence of the cerebrospinal fluid space in the left anterior, middle cranial fossa, possibly representing an arachnoid cyst or sequela of atrophy. Importantly, there were no radiographic signs of osteopetrosis or dysostosis multiplex that can be seen in patients with *CLCN7*-related osteopetrosis. However, the patient was found to have hypogammaglobulinemia with low serum IgG and IgM immunoglobulin levels, requiring intravenous immunoglobulin replacement treatment to

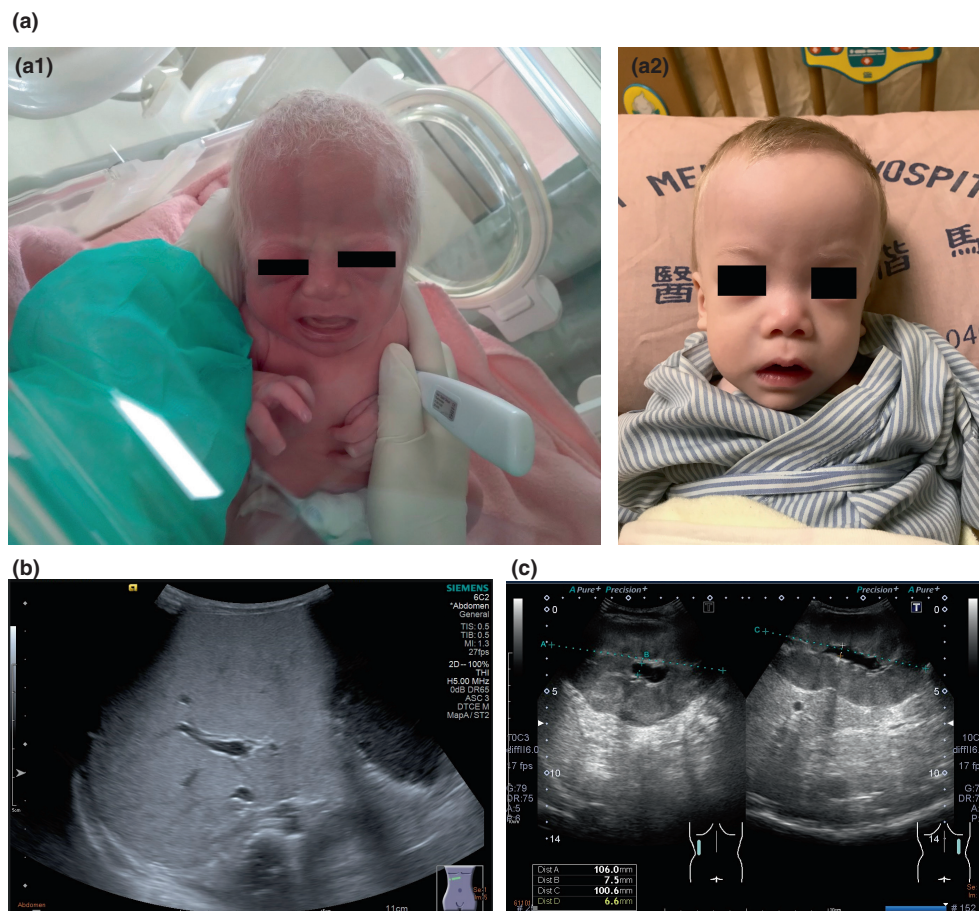


FIGURE 1 Clinical and radiological findings in the patient. (a) Patient showing hypopigmentation of the skin and hair. (a1) Birth (a2) 2-year-old (b) Abdominal ultrasonography demonstrating diffuse and homogeneous increased echogenicity of the liver. (c) Renal ultrasonography showing bilateral nephromegaly with increased echogenicity and poor corticomedullary differentiation.

prevent infections. A standard peripheral blood smear test was performed by a clinical hematopathologist to further analyze the white blood cells and evaluate the hypogammaglobulinemia. Whole-exome sequencing was also conducted on a research basis to determine the underlying genetic causes of the constellation of albinism, failure to thrive, global developmental delays, and hypogammaglobulinemia in this proband.

2.2 | Blood smear procedure

Peripheral blood smears are commonly performed as part of a routine complete blood count to visually inspect the morphology of red and white blood cells (Bain, 2006; Rodak, 2012). This study utilized standard blood smear preparation techniques as follows. A drop of whole blood was obtained by venipuncture and dispersed onto a glass microscope slide using a spreader slide held at an angled 30–45° edge. The thin blood smear was allowed to air dry thoroughly (Bain, 2006). Blood smears were fixed for 1–3 min in 100% methanol and then immersed in Wright-Giemsa polychrome stain for 30–60 s before gently rinsing in buffered water (Bain, 2006; Rodak, 2012). The stained slides were allowed to fully air dry before cover slipping and microscopy.

Microscopic analysis was carried out by an experienced hematopathologist at 100x magnification under oil immersion optics. The smears were evaluated for properties including red blood cell (RBC) morphology, white blood cell (WBC) differential counts, and platelet estimates (Bain, 2006; Rodak, 2012). Smears were also carefully assessed for abnormalities such as immature or morphologically atypical blood cells, hematologic parasites, and leukemia/lymphoma malignancies (Rodak, 2012). Manual 100-cell WBC differentials were obtained by counting and categorizing leukocytes as neutrophils, lymphocytes, monocytes, eosinophils, or basophils based on nuclear morphologic features and cytoplasmic staining characteristics (Bain, 2006).

2.3 | Whole-exome sequencing

Genomic DNA was extracted from a peripheral blood sample obtained from the proband. The proband's whole exome library was sequenced using an Illumina sequencing platform to generate 125 or 150 bp paired end reads (HiSeq4000 or NovaSeq6000). To assess the assembly quality, several metrics including sequencing depth, coverage uniformity, mismatches, base quality distribution, and insertion/deletions (indels) were evaluated in the final genome assembly. Adaptor trimming, duplicate read

removal, and alignment were carried out as described previously.

The GRCh38 primary assembly of the human reference genome was used for reading mapping and variant calling (Schneider et al., 2017). This reference contains all chromosome sequences along with unlocalized and unplaced genomic scaffolds (Genome Reference Consortium, https://www.ncbi.nlm.nih.gov/datasets/genome/GCF_000001405.40/).

To ensure high quality final genome assembly, duplicated reads were first removed as described above, and reads were realigned to the reference genome with the Burrows-Wheeler Aligner (BWA) (Li & Durbin, 2010). Variant calling performed using the Genome Analysis Toolkit (GATK) involved additional steps of indel realignment, base quality score recalibration, and removal of remaining duplicates (Van der Auwera et al., 2013). The final consensus genome representing the proband's individual genomic variation compared to the reference was assembled from the filtered, processed sequencing reads following GATK best practices guidelines (Van der Auwera et al., 2013).

Assessment and interpretation of variants was performed manually or with the Varsome clinical genome interpretation tool in accordance with American College of Medical Genetics and Genomics (ACMG) standards and guidelines for classification of pathogenic or likely pathogenic variants (Richards et al., 2015).

2.4 | Sequence data processing and analysis

The raw genomic sequencing reads generated from the proband were assessed for quality control (QC) and adaptor trimming prior to downstream analysis. Briefly, the FastQC tool (v0.11.9) was utilized to analyze per base sequence quality and other metrics to confirm sufficiently high-quality scores across bases in the raw reads (Andrews et al., 2010). Adaptor trimming to remove Illumina sequencing adaptors was then performed using the Cutadapt software (v2.5) (Martin et al., 2011). In addition, duplicate read pairs were identified by the sequencing platform and removed early in the analysis pipeline using the Picard Toolkit (v2.23.0) to avoid counting multiply mapped reads (Picard Toolkit, n.d.). The reads were not explicitly filtered based on Phred quality score thresholds or nucleotide length given the overall high data quality, making such filtering unnecessary.

Read alignment of the preprocessed sequencing data to the GRCh38 human reference genome was carried out using the Burrows-Wheeler Aligner (BWA-MEM v0.7.17)

(Li & Durbin, 2010). Variant calling was performed following Genome Analysis Toolkit (GATK v4.1.9.0) best practices guidelines (Van der Auwera et al., 2013), including marking duplicates, base quality score recalibration, and final variant calling across the exome using HaplotypeCaller in GATK. Identified coding variants were then filtered based on population minor allele frequencies and predicted functional consequences to identify rare, potentially pathogenic variants for further analysis and interpretation.

3 | RESULTS

Upon review by a hematopathologist, the Wright-Giemsa stained peripheral blood smear from the proband revealed a marked lymphocytosis with many atypical appearing lymphocytes (Figure 2). At high magnification, these cells were enlarged with lobulated nuclear contours and abundant cytoplasm containing multiple variably sized vacuoles. The lymphocytes with irregular nuclear morphology and cytoplasmic vacuolization are consistent with a reactive lymphocytosis in this clinical setting.

Analysis of the proband's whole-exome sequencing data revealed a heterozygous de novo variant in *CLCN7* (c.2144A>G [p.Tyr715Cys], GenBank: NM_001287.5) that was absent from both parental exomes (Figure 3). *CLCN7* encodes a member of the voltage-gated chloride channel protein family that includes chloride channels and chloride/proton exchangers (Jentsch, 2007; Jentsch et al., 2005; Kieferle et al., 1994; Steinmeyer et al., 1991; Thiemann et al., 1992; Uchida et al., 1994). Following ACMG criteria (Richards et al., 2015), this *CLCN7* missense variant was classified as a pathogenic variant based on its rarity in population databases, de novo occurrence, location in a critical functional domain, and demonstration of its

functional impact in previous mechanistic study (Nicoli et al., 2019).

4 | DISCUSSION

Nicoli et al. (2019) previously reported two similar cases involving a 22-month-old Caucasian girl and a 14-month-old Ghanaian boy who presented with shared features of hypopigmentation, hepatosplenomegaly, and delayed myelination and psychomotor development. Genetic analysis in these published cases revealed the identical de novo heterozygous missense mutation c.2144A>G (p.Tyr715Cys) (NM_001287.5) located in exon 23 of the *CLCN7* gene. This variant resulted in substitution of a cysteine for a highly conserved tyrosine residue at position 715 within the C-terminal cytoplasmic domain of CLC-7. This exact *CLCN7* mutation was absent in the unaffected parents in each case and has not been reported in major population genetic databases, including ExAC, gnomAD, ESP, and EVS, indicating it almost certainly represents a sporadic de novo mutation.

Functional studies conducted by Nicoli et al. (2019) revealed a 3-fold increase in outwardly rectifying chloride currents in *Xenopus laevis* oocytes expressing the mutant Y715C *CLCN7* channel compared to those expressing wild-type *CLCN7*. Electron microscopy of patient-derived fibroblasts demonstrated pathologically enlarged single- and double-membrane cytoplasmic vacuoles containing debris, reminiscent of lysosomes. Quantitative live cell imaging showed increased lysosomal acidity and enhanced accumulation of acidotropic lysosomal dyes in patient fibroblasts, indicating a reduction in lysosomal pH. Intriguingly, the vacuolar phenotype could be partially replicated in control fibroblasts by exogenous overexpression of the Y715C mutant *CLCN7* construct. Treatment with chloroquine, a lysosomotropic alkalinizing agent,

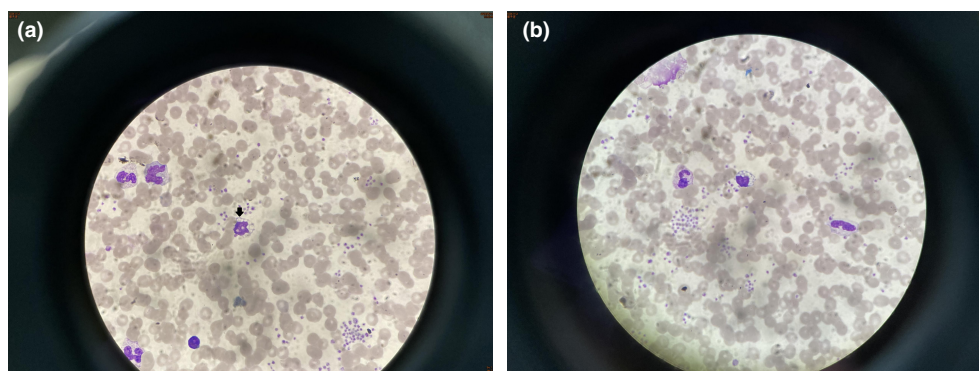


FIGURE 2 Peripheral blood smear from the proband demonstrating lymphocytosis with atypical lymphocyte morphology (Wright-Giemsa stain). (a) and (b) High magnification images (100× oil immersion) showing reactive lymphocytes with lobulated nuclei and numerous cytoplasmic vacuoles of varying sizes (indicated by arrows).

CLCN7(NM_001287.5):c.2144A>G

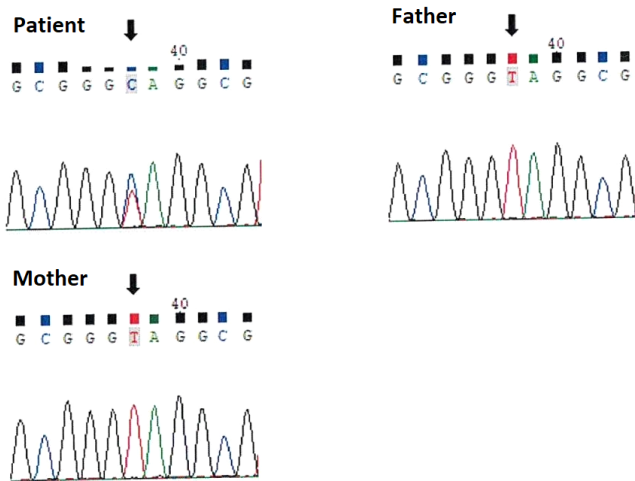


FIGURE 3 Targeted Sanger sequencing was also performed on DNA extracted from blood samples of family members.

was able to increase lysosomal pH and reduce cytoplasmic vacuoles in the probands' cells in a dose-dependent manner. Taken together, these functional studies provide compelling evidence that the Y715C mutation leads to impaired CLCN7 chloride/proton exchange function, resulting in defective lysosomal acidification and pathologic cytoplasmic vacuolization. Of note, while enlarged vacuoles were observed in fibroblasts in the Nicoli et al. (2019) report, we observed similar vacuoles accumulating in the lymphocytes of our proband, highlighting potential cell type differences. Other reports have documented the formation of large cytoplasmic vacuoles following treatment with vacuolin-1 to impair lysosomal degradation (Lu et al., 2014) or overexpression of LIMPII to disrupt lysosomal trafficking (Kuronita et al., 2002). Further studies are warranted to investigate the mechanistic basis by which decreased lysosomal pH could induce intracellular vacuole formation and determine the origin of these vacuoles across cell types.

The findings by Nicoli et al. (2019) revealed patient fibroblasts harboring the activating Y715C mutation exhibited a reduced lysosomal pH profile, lending support to the hypothesized role of CLC-7 in directly regulating lysosomal pH—a topic that has been controversial with conflicting reports in the literature (Graves et al., 2008; Jentsch, 2007; Kasper et al., 2005; Kornak et al., 2001; Majumdar et al., 2011; Steinberg et al., 2010; Weinert et al., 2010). The extensive cellular pathology observed in the probands studied by Nicoli et al. (2019) highlights that even a subtle reduction of approximately 0.2 pH units (from 4.4 to 4.2) in lysosomal pH, reflecting around a 60% increase in lysosomal free proton concentration, can profoundly and adversely impact numerous downstream processes and metabolic pathways. The wide array

of clinical phenotypes and cellular abnormalities seen, including features resembling the sequelae of many established lysosomal storage diseases, implies there is impaired activity of multiple lysosomal hydrolase enzymes that require an acidic pH optimum to function correctly at the lower lysosomal pH resulting from disrupted CLC-7 activity. However, direct quantification of specific lysosomal enzyme activities in patient fibroblasts was inconclusive using standard assays because these are performed in artificially buffered solutions at the optimal pH for each individual enzyme's activity. Alternative lysosomal enzyme quantification approaches in unbuffered solutions across a range of pH may help further clarify and quantify this relationship between pH and cellular phenotype. Nevertheless, the generalized hypopigmentation and aberrant melanosome morphology observed by light and electron microscopy in the probands studied by Nicoli et al. (2019) strongly supports the functional importance of melanosomal pH homeostasis in normal melanogenesis (Ancans et al., 2001).

In contrast to the previous cases reported by Nicoli et al. (2019), the patient described in our current case report prominently exhibited hypogammaglobulinemia, which was characterized by significantly low levels of IgM and IgG immunoglobulin classes. Recent research studies have demonstrated the critical importance of proper lysosomal acidification for normal B cell maturation, B cell receptor trafficking, plasma cell differentiation, and antibody production (Chen et al., 2014; Crotzer & Blum, 2005; Fehr et al., 1970; Rocha & Neefjes, 2008; Sandoval et al., 2018). The lysosomal pH has been shown to be a key factor enabling antigen processing and loading onto MHC class II proteins in B cells (Crotzer & Blum, 2005; Rocha & Neefjes, 2008). Additionally, antibody-secreting plasma cells require an acidic lysosomal compartment both for efficient synthesis of enormous amounts of immunoglobulin proteins and also for correct immunoglobulin protein folding and QC prior to secretion (Fehr et al., 1970; Trivedi et al., 2006).

Certain congenital lysosomal storage disorders caused by defects in lysosomal acidification, such as Mucopolysaccharidosis type II (I-cell disease) and Mucopolysaccharidosis type III (Pseudo-Hurler polydystrophy), as well as Chédiak-Higashi syndrome, can frequently manifest with hypogammaglobulinemia and increased infection susceptibility along with other systemic features (Kypri et al., 2007; Otomo et al., 2011). The underlying genetic mutations in these diseases lead to impaired lysosomal pH homeostasis through various mechanisms, but ultimately converge on disrupting B cell maturation and plasma cell function due to the lysosomal defects. Additionally, some acquired conditions such as multiple myeloma have been shown to impair

lysosomal acidification, which correlates with the ability of the neoplastic plasma cells to produce monoclonal immunoglobulins, potentially owing to intracellular accumulation of misfolded immunoglobulin proteins overloading the lysosomal compartment (Carrino et al., 2019; Nicastrì et al., 2002). Therapeutic modulation of lysosomal pH using agents such as chloroquine has shown promise in partially restoring immunoglobulin concentrations in some patients with certain congenital lysosomal storage diseases (Martinez et al., 2020), highlighting the reversible nature of this pathophysiology. These findings point to intriguing new therapeutic opportunities using lysosomal modulators to treat the antibody deficiency and increased infections associated specifically with lysosomal acidification defects.

The tissue and cellular distribution of *CLCN7* expression is indeed intriguing and may provide insights into the multisystem pathologies observed in our patient. As you astutely point out, several studies have demonstrated that *CLCN7* mRNA and protein are highly expressed in melanocytes, neurons, and monocyte-derived cells such as macrophages and Kupffer cells, while expression appears to be lower in lymphocytes (Kasper et al., 2005; Kornak et al., 2001; Weinert et al., 2010).

The high expression in melanocytes aligns with the critical role of *CLCN7* in regulating melanosomal pH and supports the hypopigmentation phenotype observed in our patient and in mice harboring the homologous *Clcn7* mutation (Nicoli et al., 2019). Similarly, the abundance of *CLCN7* in neurons, particularly in specific subpopulations like horizontal cells, may relate to the neurological manifestations of the disease such as developmental delay and myelination abnormalities. The lysosomal storage phenotype may be exacerbated in highly phagocytic cells like macrophages and Kupffer cells, where the degradative capacity of lysosomes is essential for processing ingested material.

The relatively lower expression of *CLCN7* in B cells is noteworthy, as it suggests that the hypogammaglobulinemia in our patient may not be a direct consequence of the *CLCN7* dysfunction within B cells themselves. Rather, it is possible that disrupted lysosomal function in other cell types that interact with or support B cells, such as macrophages or dendritic cells, could indirectly impair B cell maturation or function. Alternatively, *CLCN7* may be more selectively upregulated in specific B cell subsets (e.g., plasma cells) or during particular phases of B cell differentiation, which could reconcile an important physiological role for *CLCN7* in B cells with the ostensibly low expression at a bulk population level.

Examining *CLCN7* expression patterns in human B cell subsets and determining the impact of *CLCN7* mutations

on B cell and plasma cell function are important areas for future investigation. Delineating the cell type-specific consequences of *CLCN7* mutations and how they culminate in the aggregate clinical phenotype could advance our understanding of the underlying disease mechanisms and pinpoint the most consequential cellular targets for therapeutic intervention.

We acknowledge several limitations of our study. One important limitation is the lack of neonatal immunoglobulin data for the patient. As the patient was born at an outside hospital and only transferred to our institution at around 2 years of age, we were unable to assess the patient's baseline IgG and IgM levels at birth. This is particularly relevant as maternal IgG is actively transferred to the fetus during pregnancy, and IgG levels are normally highest at birth before declining over the first few months of life as maternal antibodies are catabolized (Heininger et al., 2009; Leuridan et al., 2011; Mankarious et al., 1988). In contrast, IgM does not cross the placenta, and neonatal IgM levels are normally low (Ballow et al., 1986; Wilson et al., 1986).

Without access to neonatal data, we cannot rule out the possibility that the patient may have had normal or near-normal IgG levels that subsequently fell as maternal antibodies waned, which would suggest a different tempo of antibody decline compared to the typical transient hypogammaglobulinemia of infancy. Alternatively, the patient may have had low IgG and/or IgM levels even at birth, which could point to an underlying primary immunodeficiency. Delineating these possibilities would provide important insights into the mechanism and timeline of the hypogammaglobulinemia. We were unable to obtain the original neonatal records after multiple attempts, reflecting the challenges of piecing together a complete medical history for patients with rare diseases who have received care at multiple institutions. Prospective tracking of immunoglobulin trajectories from birth in future cases could be very informative for understanding the clinical history and classifying these disorders.

5 | CONCLUSIONS

In summary, tightly regulated lysosomal acidification within a narrow physiological range is essential for supporting normal B cell maturation, immunoglobulin production, plasma cell function, and adaptive humoral immunity. Subtle disruptions in lysosomal pH homeostasis can result in a spectrum of immunoglobulin deficiencies with increased susceptibility to infections. Further elucidating the molecular mechanisms regulating lysosomal pH will enable improved understanding, diagnosis, and personalized management of this subset of inborn errors

of immunity. Our case report demonstrates that the novel gain-of-function *CLCN7* mutation, p.Tyr715Cys, underlies a complex human disease phenotype including hypopigmentation, organomegaly, developmental delay, hypogammaglobulinemia with lymphocyte vacuoles, and CNS demyelination in the absence of the osteopetrosis typically associated with *CLCN7* loss-of-function mutations. These clinical findings underscore the intricate role of ClC-7 in meticulously regulating lysosomal pH within a narrow range to support diverse cellular processes. The ability of chloroquine treatment to reverse the abnormal cellular phenotype provides a potential precision therapy for patients harboring this specific mutation, while highlighting the value of understanding the molecular factors regulating lysosomal pH homeostasis for discovering new treatment strategies. This case also motivates future investigations into the pathophysiological mechanisms connecting disrupted lysosomal pH regulation with membrane trafficking defects and cytoplasmic vacuolization across cell types.

AUTHOR CONTRIBUTIONS

C.L.L. wrote the initial draft of the manuscript. Y.W.C., S.P.L., J.D.T., H.C.L., T.C.Y., and L.C.F. were involved in patient follow-up care. S.P.L., J.D.T., and H.Y.L. assisted with drafting the manuscript. T.C.Y. conducted the biochemical assays and reviewed the manuscript. N.C.L. performed patient screening and provided critical revisions. All authors read and approved the final submitted version of the manuscript.

ACKNOWLEDGMENTS

The authors would like to express their gratitude to all the staff members who contributed to this study and the patients who participated in this research.

FUNDING INFORMATION

This study was supported by research grants from the MacKay Memorial Hospital (MMH-MM-113-13, MMH-E-113-13, MMH-MM-112-14, MMH-E-112-13, and MMH-E-111-13) and the National Science and Technology Council, Executive Yuan, Taiwan (NSTC-112-2314-B-195-014-MY3, NSTC-112-2811-B-195-001, NSTC-112-2314-B-195-003, NSTC-111-2314-B-195-017, NSTC-111-2811-B-195-002, NSTC-111-2811-B-195-001, NSTC-110-2314-B-195-014, NSTC-110-2314-B-195-010-MY3, and NSTC-110-2314-B-195-029).

CONFLICT OF INTEREST STATEMENT

The authors declare that they have no conflicts of interest.

DATA AVAILABILITY STATEMENT

The data supporting the findings of this study are available from the corresponding author upon reasonable request.

ETHICS STATEMENT

This study was conducted according to the guidelines of the Declaration of Helsinki and approved by the Institutional Review Board of MacKay Memorial Hospital (approval number 21MMHIS109e on 2021/10/01). Following their ethics review, the hospital review board affirmed the ethical compliance of the study and authorized the publication of the findings.

INFORMED CONSENT

Written informed consent has been obtained from the patient's parents to publish this paper.

ORCID

Chung-Lin Lee  <https://orcid.org/0000-0001-8178-6938>

Hsiang-Yu Lin  <https://orcid.org/0000-0002-9619-0990>

Hung-Chang Lee  <https://orcid.org/0000-0002-5011-7499>

REFERENCES

- Ancans, J., Tobin, D. J., Hoogduijn, M. J., Smit, N. P., Wakamatsu, K., & Thody, A. J. (2001). Melanosomal pH controls rate of melanogenesis, eumelanin/phaeomelanin ratio and melanosome maturation in melanocytes and melanoma cells. *Experimental Cell Research*, 268(1), 26–35. <https://doi.org/10.1006/excr.2001.5260>
- Andrews, S. FastQC: a quality control tool for high throughput sequence data. 2010. Available online at: <http://www.bioinformatics.babraham.ac.uk/projects/fastqc/>
- Bain, B. J. (2006). *Blood cells: A practical guide* (4th ed.). Blackwell Publishing.
- Ballow, M., Cates, K. L., Rowe, J. C., Goetz, C., & Desbonnet, C. (1986). Development of the immune system in very low birth weight (less than 1500 g) premature infants: Concentrations of plasma immunoglobulins and patterns of infections. *Pediatric Research*, 20(9), 899–904. <https://doi.org/10.1203/00006450-198609000-00019>
- Bose, S., de Heus, C., Kennedy, M. E., Wang, F., Jentsch, T. J., Klumperman, J., & Stauber, T. (2023). Impaired autophagic clearance with a gain-of-function variant of the lysosomal Cl⁻/H⁺ exchanger ClC-7. *Biomolecules*, 13(2), 1799. <https://doi.org/10.3390/biom13021799>
- Carrino, M., Quotti Tubi, L., Fregnani, A., Capello, M., Bernardoni, P., Albano, F., Viganò, C., Locatelli, S. L., Frasson, C., Raiteri, E., Manieri, L., Rocco, D., Omedè, P., Pesce, E. R., Biciato, S., Tagliaferri, P., & Chiaromonte, R. (2019). Prosurvival autophagy is regulated by protein kinase CK1 α in multiple myeloma. *Cell Death Discovery*, 5, 98. <https://doi.org/10.1038/s41420-019-0192-6>
- Chen, M., Hong, M. J., Sun, H., Wang, L., Shi, X., Gilbert, B. E., Corry, D. B., Kheradmand, F., & Zheng, P. (2014). Essential role for autophagy in the maintenance of immunological memory against influenza infection. *Nature Medicine*, 20(5), 503–510. <https://doi.org/10.1038/nm.3521>
- Crotzer, V. L., & Blum, J. S. (2005). Autophagy and intracellular surveillance: Modulating MHC class II antigen presentation with stress. *Proceedings of the National Academy of Sciences of the*

- United States of America, 102(19), 7779–7780. <https://doi.org/10.1073/pnas.0503361102>
- Devuyt, O., Christie, P. T., Courtoy, P. J., Beauwens, R., & Thakker, R. V. (1999). Intra-renal and subcellular distribution of the human chloride channel, CLC-5, reveals a pathophysiological basis for Dent's disease. *Human Molecular Genetics*, 8(2), 247–257. <https://doi.org/10.1093/hmg/8.2.247>
- Fehr, K., LoSpalluto, J., & Ziff, M. (1970). Degradation of immunoglobulin G by lysosomal acid proteases. *The Journal of Immunology*, 105(4), 973–983. <https://doi.org/10.4049/jimmunol.105.4.973>
- Graves, A. R., Curran, P. K., Smith, C. L., & Mindell, J. A. (2008). The Cl⁻/H⁺ antiporter CLC-7 is the primary chloride permeation pathway in lysosomes. *Nature*, 453(7196), 788–792. <https://doi.org/10.1038/nature06907>
- Hamer, I., Van Beersel, G., Arnould, T., & Jadot, M. (2012). Lipids and lysosomes. *Current Drug Metabolism*, 13(10), 1371–1387. <https://doi.org/10.2174/138920012802850064>
- Heininger, U., Riffelmann, M., Leineweber, B., & Wirsing von Koenig, C. H. (2009). Maternally derived antibodies against Bordetella pertussis antigens pertussis toxin and filamentous hemagglutinin in preterm and full term newborns. *The Pediatric Infectious Disease Journal*, 28(5), 443–445. <https://doi.org/10.1097/INF.0b013e318193ead7>
- Jentsch, T. J. (2007). Chloride and the endosomal-lysosomal pathway: Emerging roles of CLC chloride transporters. *The Journal of Physiology*, 578(Pt 3), 633–640. <https://doi.org/10.1113/jphysiol.2006.124719>
- Jentsch, T. J., Poët, M., Fuhrmann, J. C., & Zdebik, A. A. (2005). Physiological functions of CLC Cl⁻ channels gleaned from human genetic disease and mouse models. *Annual Review of Physiology*, 67, 779–807. <https://doi.org/10.1146/annurev.physiol.67.032003.153247>
- Kasper, D., Planells-Cases, R., Fuhrmann, J. C., Scheel, O., Zeitz, O., Ruether, K., Schmitt, A., Poët, M., Steinfeld, R., Schweizer, M., Kornak, U., & Jentsch, T. J. (2005). Loss of the chloride channel CLC-7 leads to lysosomal storage disease and neurodegeneration. *The EMBO Journal*, 24(5), 1079–1091. <https://doi.org/10.1038/sj.emboj.7600576>
- Kieferle, S., Fong, P., Bens, M., Vandewalle, A., & Jentsch, T. J. (1994). Two highly homologous members of the CLC chloride channel family in both rat and human kidney. *Proceedings of the National Academy of Sciences of the United States of America*, 91(24), 6943–6947. <https://doi.org/10.1073/pnas.91.15.6943>
- Kornak, U., Kasper, D., Bosl, M. R., Kaiser, E., Schweizer, M., Schulz, A., Friedrich, W., Dellling, G., & Jentsch, T. J. (2001). Loss of the CLC-7 chloride channel leads to osteopetrosis in mice and man. *Cell*, 104(2), 205–215. [https://doi.org/10.1016/s0092-8674\(01\)00206-9](https://doi.org/10.1016/s0092-8674(01)00206-9)
- Kuronita, T., Eskelinen, E. L., Fujita, H., Saftig, P., Himeno, M., & Tanaka, Y. (2002). A role for the lysosomal membrane protein LAMP2 in the biogenesis and maintenance of endosomal and lysosomal morphology. *Journal of Cell Science*, 115(Pt 21), 4117–4131. <https://doi.org/10.1242/jcs.00127>
- Kypri, E., Schmauch, C., Maniak, M., & De Lozanne, A. (2007). The BEACH protein LvsB is localized on lysosomes and postlysosomes and limits their fusion with early endosomes. *Traffic (Copenhagen, Denmark)*, 8(7), 774–783. <https://doi.org/10.1111/j.1600-0854.2007.00566.x>
- Lange, P. F., Wartosch, L., Jentsch, T. J., & Fuhrmann, J. C. (2006). CLC-7 requires Ostm1 as a beta-subunit to support bone resorption and lysosomal function. *Nature*, 440(7084), 220–223. <https://doi.org/10.1038/nature04535>
- Leuridan, E., Hens, N., Peeters, N., de Witte, L., Van der Meeren, O., & Van Damme, P. (2011). Effect of a prepregnancy pertussis booster dose on maternal antibody titers in young infants. *The Pediatric Infectious Disease Journal*, 30(7), 608–610. <https://doi.org/10.1097/INF.0b013e3182093814>
- Li, H., & Durbin, R. (2010). Fast and accurate long-read alignment with burrows-wheeler transform. *Bioinformatics*, 26(5), 589–595. <https://doi.org/10.1093/bioinformatics/btp698>
- Lu, Y., Dong, S., Hao, B., Li, C., Zhu, K., Guo, W., Wang, Q., Cheong, K. L., Wu, Y., Zheng, M., Chen, X., Wang, L., Li, N., Tan, T., Zeng, R., Chen, L., & Liu, P. (2014). Vacuolin-1 potently and reversibly inhibits autophagosome-lysosome fusion by activating RAB5A. *Autophagy*, 10(11), 1895–1905. <https://doi.org/10.4161/auto.34398>
- Majumdar, A., Capetillo-Zarate, E., Cruz, D., Gouras, G. K., & Maxfield, F. R. (2011). Degradation of Alzheimer's amyloid fibrils by microglia requires delivery of CLC-7 to lysosomes. *Molecular Biology of the Cell*, 22(10), 1664–1676. <https://doi.org/10.1091/mbc.e10-09-0745>
- Mankariou, S., Lee, M., Fischer, S., Pyun, K. H., Ochs, H. D., Oxelius, V. A., & Wedgwood, R. J. (1988). The half-lives of IgG subclasses and specific antibodies in patients with primary immunodeficiency who are receiving intravenously administered immunoglobulin. *The Journal of Laboratory and Clinical Medicine*, 112(5), 634–640.
- Martin, M. (2011). Cutadapt removes adapter sequences from high-throughput sequencing reads. *EMBnet journal*, 17(1), 10–12. <https://doi.org/10.14806/ej.17.1.200>
- Martinez, G. P., Zabaleta, M. E., Di Giulio, C., Charris, J. E., & Mijares, M. R. (2020). The role of chloroquine and hydroxychloroquine in immune regulation and diseases. *Current Pharmaceutical Design*, 26(35), 4467–4485. <https://doi.org/10.2174/138161282666201030131848>
- Mindell, J. A. (2012). Lysosomal acidification mechanisms. *Annual Review of Physiology*, 74, 69–86. <https://doi.org/10.1146/annurev-physiol-012110-142317>
- Mohammad-Panah, R., Ackerley, C., Rommens, J., Choudhury, M., Wang, Y., & Bear, C. E. (2002). The chloride channel CLC-4 co-localizes with cystic fibrosis transmembrane conductance regulator and may mediate chloride flux across the apical membrane of intestinal epithelia. *The Journal of Biological Chemistry*, 277(8), 566–574. <https://doi.org/10.1074/jbc.M108851200>
- Nicastri, A. L., Prado, M. J., Dominguez, W. V., & Prado, E. B. (2002). Nephrotoxicity of Bence-Jones proteins: Interference in renal epithelial cell acidification. *Brazilian Journal of Medical and Biological Research*, 35, 357–360. <https://doi.org/10.1590/S0100-879X2002000400003>
- Nicoli, E. R., Weston, M. R., Hackbarth, M., Lee, B. B., Weisbrod, B. L., Marshall, M. J., Lee, C. C., González-Perrett, S., Luz, S., Wang, F., Feldman, E. L., Yang, J. J., Schotanus, M. P., van den Heuvel, L. P., Poët, M., Wang, X., Kornak, U., Rodenburg, R. J., Willemsen, M. A., ... Gehrig, A. (2019). Lysosomal storage and albinism due to effects of a de novo CLCN7 variant on lysosomal acidification. *The American Journal of Human Genetics*, 104(6), 1127–1138. <https://doi.org/10.1016/j.ajhg.2019.04.001>

- Otomo, T., Higaki, K., Nanba, E., Ozono, K., & Sakai, N. (2011). Lysosomal storage causes cellular dysfunction in mucopolidosis II skin fibroblasts. *The Journal of Biological Chemistry*, 286(40), 35283–35290. <https://doi.org/10.1074/jbc.M111.253696>
- Picard Toolkit Broad institute, GitHub repository. <http://broadinstitute.github.io/picard/>
- Poët, M., Kornak, U., Schweizer, M., Zdebik, A. A., Scheel, O., Hoelter, S., Wurst, W., Schmitt, A., Fuhrmann, J. C., Planells-Cases, R., Mole, S. E., Hübner, C. A., & Jentsch, T. J. (2006). Lysosomal storage disease upon disruption of the neuronal chloride transport protein CLC-6. *Proceedings of the National Academy of Sciences of the United States of America*, 103(51), 13854–13859. <https://doi.org/10.1073/pnas.0606137103>
- Richards, S., Aziz, N., Bale, S., Bick, D., das, S., Gastier-Foster, J., Grody, W. W., Hegde, M., Lyon, E., Spector, E., Voelkerding, K., Rehm, H. L., & ACMG Laboratory Quality Assurance Committee. (2015). Standards and guidelines for the interpretation of sequence variants: A joint consensus recommendation of the American College of Medical Genetics and Genomics and the Association for Molecular Pathology. *Genetics in Medicine*, 17(5), 405–424. <https://doi.org/10.1038/gim.2015.30>
- Rocha, N., & Neefjes, J. (2008). MHC class II molecules on the move for successful antigen presentation. *The EMBO Journal*, 27(1), 1–5. <https://doi.org/10.1038/sj.emboj.7601945>
- Rodak, B. F. (2012). *Hematology: Clinical principles and applications* (4th ed.). Elsevier Health Sciences.
- Sandoval, H., Kodali, S., & Wang, J. (2018). Regulation of B cell fate, survival, and function by mitochondria and autophagy. *Mitochondrion*, 41, 58–65. <https://doi.org/10.1016/j.mito.2017.10.007>
- Schneider, V. A., Graves-Lindsay, T., Howe, K., Bouk, N., Chen, H. C., Kitts, P. A., Murphy, T. D., Pruitt, K. D., Thibaud-Nissen, F., Albracht, D., Fulton, R. S., Kremitzki, M., Magrini, V., Markovic, C., McGrath, S., Steinberg, K. M., Auger, K., Chow, W., Collins, J., ... Church, D. M. (2017). Evaluation of GRCh38 and de novo haploid genome assemblies demonstrates the enduring quality of the reference assembly. *Genome Research*, 27(5), 849–864. <https://doi.org/10.1101/gr.213611.116>
- Steinberg, B. E., Huynh, K. K., Brodovitch, A., Jabs, S., Stauber, T., Jentsch, T. J., & Grinstein, S. (2010). A cation counterflux supports lysosomal acidification. *The Journal of Cell Biology*, 189(7), 1171–1186. <https://doi.org/10.1083/jcb.200911083>
- Steinmeyer, K., Ortlund, C., & Jentsch, T. J. (1991). Primary structure and functional expression of a developmentally regulated skeletal muscle chloride channel. *Nature*, 354(6352), 301–304. <https://doi.org/10.1038/354301a0>
- Stobrawa, S. M., Breiderhoff, T., Takamori, S., Engel, D., Schweizer, M., Zdebik, A. A., Bösl, M. R., Ruether, K., Jahn, H., Draguhn, A., Jahn, R., & Jentsch, T. J. (2001). Disruption of CLC-3, a chloride channel expressed on synaptic vesicles, leads to a loss of the hippocampus. *Neuron*, 29(1), 185–196. [https://doi.org/10.1016/s0896-6273\(01\)00189-1](https://doi.org/10.1016/s0896-6273(01)00189-1)
- Thiemann, A., Gründer, S., Pusch, M., & Jentsch, T. J. (1992). A chloride channel widely expressed in epithelial and non-epithelial cells. *Nature*, 356(6364), 57–60. <https://doi.org/10.1038/356057a0>
- Trivedi, V., Zhang, S. C., Castoreno, A. B., Stockinger, W., Shieh, E. C., Vyas, J. M., & Frickel, E. M. (2006). Immunoglobulin G signaling activates lysosome/phagosome docking. *Proceedings of the National Academy of Sciences of the United States of America*, 103(48), 18226–18231. <https://doi.org/10.1073/pnas.0608915103>
- Uchida, S., Sasaki, S., Furukawa, T., Hiraoka, M., Imai, T., Hirata, Y., & Marumo, F. (1994). Molecular cloning of a chloride channel that is regulated by dehydration and expressed predominantly in kidney medulla. *The Journal of Biological Chemistry*, 269(31), 19192–19198. [https://doi.org/10.1016/S0021-9258\(17\)32384-8](https://doi.org/10.1016/S0021-9258(17)32384-8)
- Van der Auwera, G. A., Carneiro, M. O., Hartl, C., Poplin, R., Del Angel, G., Levy-Moonshine, A., Jordan, T., Shakir, K., Roazen, D., Thibault, J., & Banks, E. (2013). From FastQ data to high confidence variant calls: The genome analysis toolkit best practices pipeline. *Current Protocols in Bioinformatics*, 43, 11. <https://doi.org/10.1002/0471250953.bi1110s43>
- Weinert, S., Jabs, S., Supanchart, C., Schweizer, M., Kimber, N., Richter, M., Rademann, J., Stauber, T., Kornak, U., & Jentsch, T. J. (2010). Lysosomal pathology and osteopetrosis upon loss of H⁺-driven lysosomal Cl⁻ accumulation. *Science (New York, N.Y.)*, 328(5984), 1401–1403. <https://doi.org/10.1126/science.1188072>
- Wilson, C. B., Westall, J., Johnston, L., Lewis, D. B., Dower, S. K., & Alpert, A. R. (1986). Decreased production of interferon-gamma by human neonatal cells. Intrinsic and regulatory deficiencies. *The Journal of Clinical Investigation*, 77(3), 860–867. <https://doi.org/10.1172/JCI112383>
- Xiong, J., & Zhu, M. X. (2016). Regulation of lysosomal ion homeostasis by channels and transporters. *Science China. Life Sciences*, 59(8), 777–791. <https://doi.org/10.1007/s11427-016-5090-x>

How to cite this article: Lee, C.-L., Chang, Y.-W., Lin, H.-Y., Lee, H.-C., Yeh, T.-C., Fang, L.-C., Lee, N.-C., Tsai, J.-D., & Lin, S.-P. (2024). Multisystem disorder associated with a pathogenic variant in *CLCN7* in the absence of osteopetrosis. *Molecular Genetics & Genomic Medicine*, 12, e2494. <https://doi.org/10.1002/mgg3.2494>